Science of the Total Environment 506–507 (2015) 422–429

Contents lists available at ScienceDirect

Science of the Total Environment

journal homepage: www.elsevier.com/locate/scitotenv

Diurnal emissivity dynamics in bare *versus* biocrusted sand dunes

Offer Rozenstein [a], Nurit Agam [a], Carmine Serio [b], Guido Masiello [b], Sara Venafra [b], Stephen Achal [c], Eldon Puckrin [d], Arnon Karnieli [a,*]

[a] Jacob Blaustein Institutes for Desert Research, Ben-Gurion University of the Negev, Sede Boker Campus, 84990, Israel
[b] School of Engineering and CNISM, Potenza Research Unit, University of Basilicata, Potenza, Italy
[c] ITRES Research Ltd. #110, 3553 31st Street, N.W. Calgary, Alberta T2L 2K7, Canada
[d] Defence Research and Development Canada (DRDC) — Valcartier, 2459 de la Bravoure, Québec, QC G3J 1X5, Canada

HIGHLIGHTS

- A geostationary space observation of land surface emissivity dynamics was conducted.
- Diurnal emissivity variations were greater in biocrusted than in bare sands.
- The emissivity variations were caused by water vapor adsorption and evaporation.

GRAPHICAL ABSTRACT

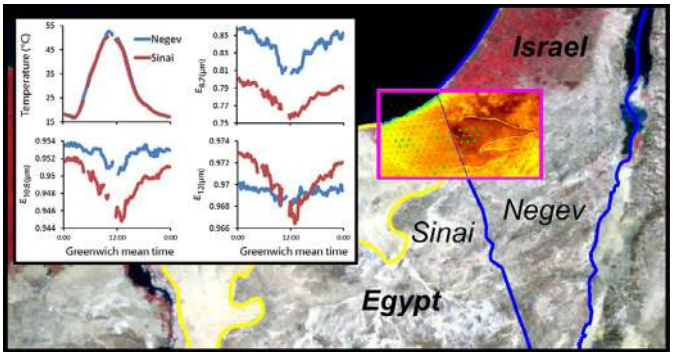

ARTICLE INFO

Article history:
Received 31 July 2014
Received in revised form 7 November 2014
Accepted 9 November 2014
Available online xxxx

Editor: Simon James Pollard

Keywords:
Thermal remote sensing
LWIR
SEVIRI
Biocrust
Sand dunes
Water vapor adsorption

ABSTRACT

Land surface emissivity (LSE) in the thermal infrared depends mainly on the ground cover and on changes in soil moisture. The LSE is a critical variable that affects the prediction accuracy of geophysical models requiring land surface temperature as an input, highlighting the need for an accurate derivation of LSE. The primary aim of this study was to test the hypothesis that diurnal changes in emissivity, as detected from space, are larger for areas mostly covered by biocrusts (composed mainly of cyanobacteria) than for bare sand areas. The LSE dynamics were monitored from geostationary orbit by the Spinning Enhanced Visible and Infrared Imager (SEVIRI) over a sand dune field in a coastal desert region extending across both sides of the Israel–Egypt political borderline. Different land-use practices by the two countries have resulted in exposed, active sand dunes on the Egyptian side (Sinai), and dunes stabilized by biocrusts on the Israeli side (Negev). Since biocrusts adsorb more moisture from the atmosphere than bare sand does, and LSE is affected by the soil moisture, diurnal fluctuations in LSE were larger for the crusted dunes in the 8.7 μm channel. This phenomenon is attributed to water vapor adsorption by the sand/biocrust particles. The results indicate that LSE is sensitive to minor changes in soil water content caused by water vapor adsorption and can, therefore, serve as a tool for quantifying this effect, which has a large spatial impact. As biocrusts cover vast regions in deserts worldwide, this discovery has repercussions for LSE estimations in deserts around the globe, and these LSE variations can potentially have considerable effects on geophysical models from local to regional scales.

* Corresponding author. Tel.: +972 8 6596855, +972 52 8795925 (mobile); fax: +972 8 6596805.
E-mail address: karnieli@bgu.ac.il (A. Karnieli).

http://dx.doi.org/10.1016/j.scitotenv.2014.11.035
0048-9697/

1. Introduction

Land surface emissivity (LSE) is the ratio between the radiance emitted by the land surface and the radiance emitted by a black body at the same temperature (Li et al., 2012, 2013a). The estimation of LSE by remote sensing in the long-wave infrared (LWIR) spectral region (8–13 μm) is mainly dependent on the surface cover (rock, soil, vegetation, *etc.*) and viewing angle (Hulley et al., 2010; Li et al., 2013a). However, LSE also nonlinearly varies according to changes in soil moisture caused by precipitation, condensation, and evaporation (Mira et al., 2007, 2010; Sanchez et al., 2011). In drylands, even small-scale changes in soil moisture that occur due to dew formation, as well as direct water vapor adsorption by the soil, can cause LSE variations (Li et al., 2012). Water vapor from the atmosphere may be directly absorbed by the soil matrix as a result of capillary condensation and/or physical adsorption. The former is the predominant mechanism when the relative humidity in the pores is high, while the latter predominates at low values of relative humidity (Philip and De Vries, 1957). Accurate LSE estimation is vital for the derivation of various surface and atmospheric variables. For instance, hydrological, climate, and weather models rely on LWIR LSE for determining the surface radiation budget (Immerzeel and Droogers, 2008; Zhou et al., 2003). In addition, retrieval of land surface temperature (LST) (Becker and Li, 1990; Li et al., 2013b; Rozenstein et al., 2014a; Wan and Dozier, 1996), monitoring land-use and land-cover change (French et al., 2008; Hulley et al., 2014), dust and aerosol properties (Li et al., 2007; Zhang et al., 2006), atmospheric water vapor content (Seemann et al., 2008), and trace gas content (Clerbaux et al., 2003) are all sensitive to the accuracy of LSE estimations.

In recent years, emphasis has been placed on the study of the temporal variations of LSE. The LSE derived from polar-orbiting satellites, having a revisit time of the same area of twice a day at best, can only reveal weather related LSE variations (Ogawa et al., 2008), while the diurnal dynamics are under-sampled (Li et al., 2012). Consequently, geostationary satellites with high-temporal resolutions are used to observe the diurnal dynamics of LSE. Previous studies analyzed images derived by the geostationary Spinning Enhanced Visible and InfraRed Imager (SEVIRI) and reported strong diurnal dynamics over deserts, especially for the 8.7 μm channel (Li et al., 2012; Masiello et al., 2013, 2014; Masiello and Serio, 2013), where emissivity in quartz reststrahlen bands is attenuated as soil moisture increases (Salisbury and D'Aria, 1992). These observations were explained by the diurnal soil moisture cycle resulting from direct water vapor adsorption by the soil throughout the late afternoon and night and the consequent evaporation over the following morning (Agam and Berliner, 2004).

Many desert surfaces worldwide are covered by biocrusts, composed of microphytes and soil granules that play a prominent role in hydrological cycles (Belnap, 2006). Biocrusts formation is a successional process, generally beginning with the primary colonization of the surface by filamentous cyanobacteria (Rozenstein et al., 2014b), followed by more photoautotrophic organisms. Thus, as biocrusts develop, the make-up of these microphytic communities evolves into diverse compositions of cyanobacteria, lichens, mosses, green algae, microfungi, and bacteria (Belnap and Lange, 2001; Karnieli et al., 1996). Biocrusts change the topsoil texture significantly by incorporating fine soil particles found *in-situ* and captured from dust into their structure (Danin and Ganor, 1991; Ram and Aaron, 2007; Zaady and Offer, 2010). The amount of water adsorbed by the soil increases with the clay content, since clay particles have a larger surface area, *i.e.*, more adsorption sites, per a given soil volume (Agam and Berliner, 2006). Thus, the incorporation of clay particles by biocrusts increases their ability to both absorb dew and adsorb water vapor from the atmosphere, compared with bare sand. In addition to this, biocrusts contain pores, which effectively increase their surface area and, thus, increase their adsorption abilities (Felde et al., 2014). It has been found that dew plays a major role in biocrust development (Rao et al., 2009; Veste et al., 2001) and also that biocrust absorbs more dew than sand (Liu et al., 2006; Pan et al., 2010; Zhang et al., 2009).

The primary aim of this study was to quantify the diurnal variations in LSE, as detected from space, over bare *vs.* biocrusted sands and to explore the different dynamics between these two ecosystems.

2. Material and methods

2.1. Study area

The northeastern Sinai region is characterized by linear sand dunes advancing from west to east, split by the Israel–Egypt political border (Fig. 1) (Roskin et al., 2012). Both the pedology and the climate are identical between the dunes in the Negev Desert on the Israeli side of the border, and the dunes in Sinai, Egypt. However, the Sinai and Negev dune fields differ in the land-use policy implemented by the two countries. Following the Israel–Egypt peace agreements in 1982, the borderline was redrawn in its current location, preventing nomadic Bedouin tribes from passing through. Traditional pastoralist activities in the Negev Desert have, therefore, ceased, while in Sinai, grazing and wood gathering activities have continued (Karnieli and Tsoar, 1995; Tsoar et al., 2008). Biocrusts are very sensitive to disturbance by human activities, but this degradation is reversible, and once anthropogenic pressure ceases the biocrusts may recover (Belnap, 1990; Kuske et al., 2012). As a result of reduced pressure, the dunes in the Negev have been covered by biocrusts and, consequently, have stabilized (except for a small active portion on the dune crest). In contrast, the trampling of the sand surface by the nomadic herds in Sinai has prevented biocrust establishment, leaving the sands exposed and the dunes active and mobile.

The differences in land-use and, thus, land-cover on both sides of the border result in a brightness contrast observed in reflective remote sensing images (Tsoar and Karnieli, 1996). This phenomenon, which can be seen from the air and from space, is caused by the higher albedo of the bright bare sand dunes in Sinai relative to the dark encrusted dunes of the Negev. Respectively, the darker surface of the Negev absorbs more sun irradiance during the day than the bright surface of Sinai resulting with the encrusted sands being warmer than the bare sands by up to 4 °C during the dry summer (Karnieli and Dall'Olmo, 2003; Qin et al., 2002a). This LST contrast between the two sides of the border is apparent in spaceborne images (Karnieli and Dall'Olmo, 2003; Qin et al., 2002a). At night, this temperature contrast subsides (Qin et al., 2002a); however, the LSE contrast across the border is evident during both daytime and nighttime (Rozenstein and Karnieli, 2015).

2.2. Climatological and meteorological conditions

The climate in the study area is characterized by an average air temperature ranging from 9 °C in January to 27 °C in August. A sharp north–south rainfall gradient stretches along a 30 km length where the border intersects the dune field. Typically, the southern area (away from the Mediterranean Sea) receives less than 100 mm of precipitation, whereas more than 140 mm may fall in the northern region (close to the shoreline) (Siegal et al., 2013). Meteorological conditions were monitored using a standard meteorological station located at the crest of a dune on the Israeli side of the border within the study area. Air temperature and relative humidity during the summer months, measured with a model HMP50 sensor (Campbell Scientific, Logan, Utah, USA), were characterized by high fluctuations between day and night (Fig. 2A). Wind speed and direction were measured with a model 03002 R.M. Young Wind Sentry sensor (Campbell Scientific, Logan, Utah, USA). The prevailing wind direction was primarily northwestern, and to a lesser extent, northern (Fig. 2B). Note that Fig. 2 presents a mean day created by averaging the variables over June and July 2013. The stronger afternoon wind, due to the sea breeze phenomenon, carrying moisture from the Mediterranean Sea inland, was the main source of moisture uptake by the soil during the dry

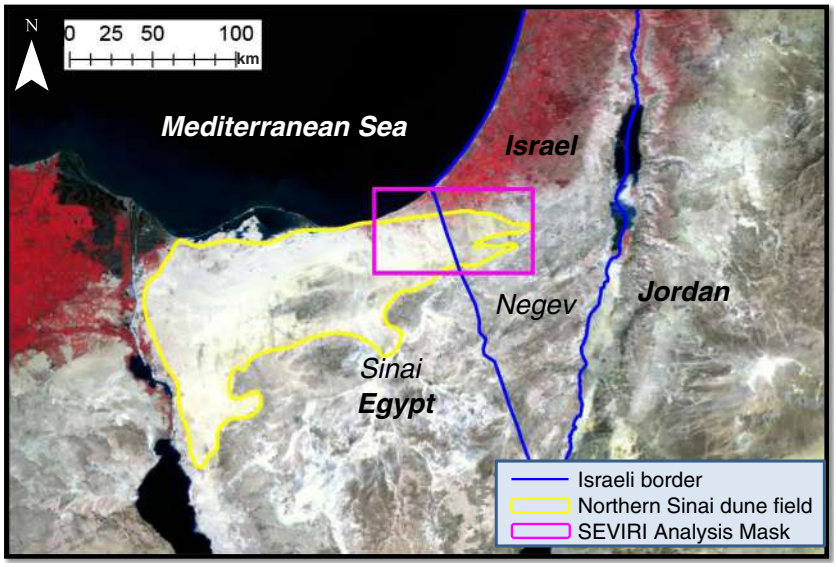

Fig. 1. MODID false color regional image (RGB = 2,1,4) of the research site acquired on February 4, 2012. The encroachment of the northern Sinai dune field across the Israeli–Egyptian political border into the northwestern Negev Desert is delineated. The rectangle represents the area of SEVIRI analysis shown in Fig. 5. (For interpretation of the references to color in this figure legend, the reader is referred to the web version of this article.)

summer months. The days selected for analysis (for reasons described in Section 2.4) were characteristic of the season in terms of air temperature, relative humidity, and wind conditions (Fig. 3).

2.3. Spectral field measurements

A portable field spectrometer with 1760 bands in the 0.7–14 μm spectral range at 8 cm^{-1} resolution (Puckrin et al., 2013) was used during a field campaign aimed at characterizing the spectral signatures of different rocks, soils, and vegetation in Israel. The Negev dune field was visited on September 19, 2013 as part of this field campaign, and the spectral signatures of key land-cover features were measured.

2.4. SEVIRI spaceborne images

Images acquired by the SEVIRI on board the geostationary Meteosat-9 satellite, over the study area during June and July 2013, were analyzed. The images were acquired at a zenith viewing angle of about 54° (ranging from 53° to 55° in the west–east direction) The data were processed using a Kalman filter for temperature–emissivity separation

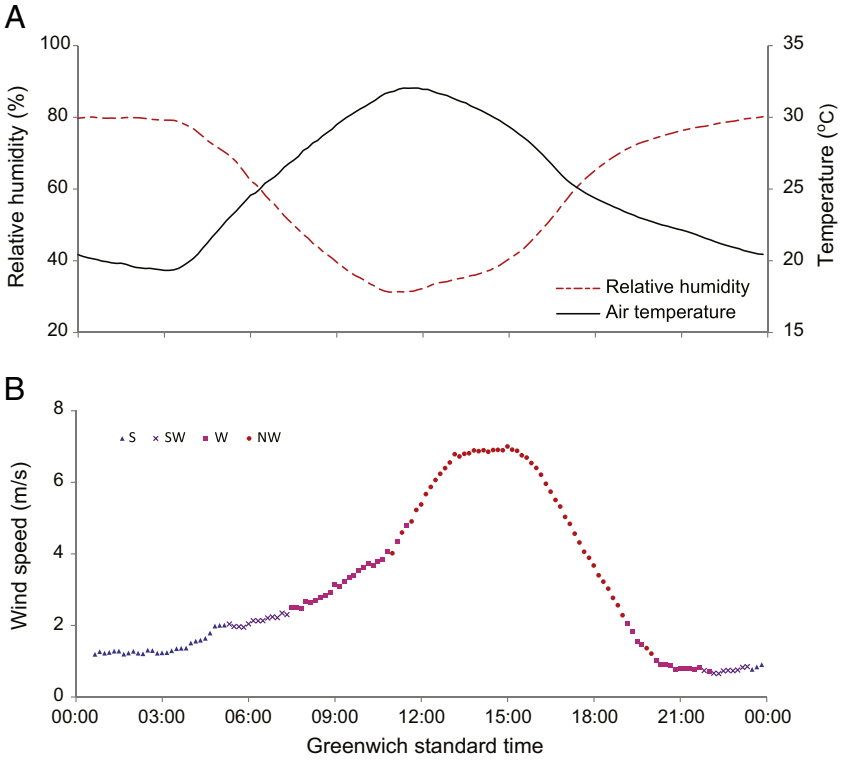

Fig. 2. Mean diurnal dynamics of A) relative humidity, and air temperature; and B) wind speed and direction for June-July 2013.

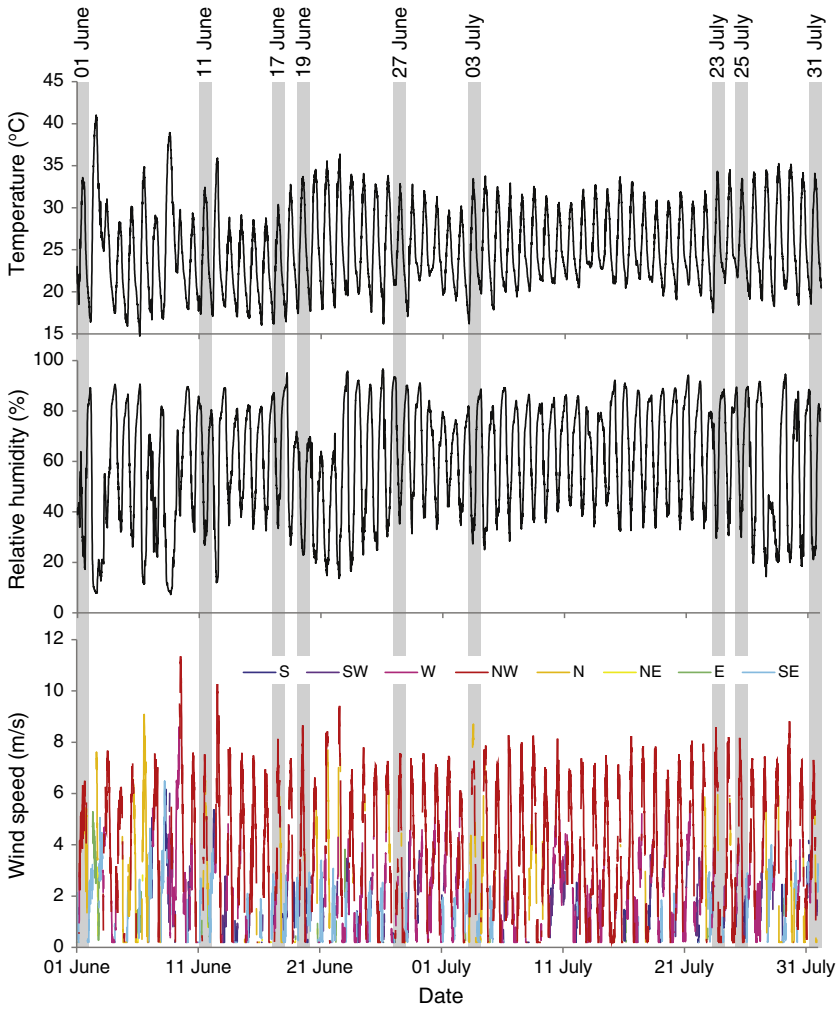

Fig. 3. Meteorological conditions at the study site during June and July 2013. Measurements were conducted at the meteorological station located within the study area (marked in Fig. 5).

in three channels centered at 8.7, 10.8, and 12 μm (Masiello et al., 2013). The Kalman filter implemented a full physical retrieval scheme that simultaneously solved the radiative transfer equation for surface temperature and emissivity. No atmospheric correction was required since the atmospheric state vector (temperature (T), water vapor (Q), and ozone (O) profile) was taken into account in the calculations. The state vector was obtained in each SEVIRI pixel through a time–space interpolation of the European Centre for Medium Range Weather Forecasts (ECMWF) analysis. For the present study, we used the ECMWF analysis on 137 vertical pressure levels with a horizontal spatial resolution of 0.125° × 0.125°. In addition, background information about the emissivity was also conveyed within the scheme, which was obtained by the University of Wisconsin (UW) Baseline FIT (BF) emissivity database (UW/BFEMIS database, http://cimss.ssec.wisc.edu/iremis/) (Seemann et al., 2008).

Masiello et al. (2013) utilized the high temporal resolution data acquired from geostationary satellites to retrieve the diurnal cycle of LST and LSE using the sequential approach of the Kalman filter. This approach's algorithm does not require increasing the dimensionality of the data space because of time accumulation of observations, while preserving the highest temporal resolution prescribed by the geostationary instrument (15 min for SEVIRI). The Masiello et al. (2013) time dimension Kalman filter approach uses a state equation to model the temporal evolution of LST and LSE. The state equation is a simple persistence with an additional stochastic term which can model the temporal variability of the surface parameters. This temporal variability is prescribed to be very low for LSE and comparatively higher for LST (see details in Masiello et al., 2013). This allows dynamically decoupling of LSE from LST, and separating the two variables from the radiative transfer equation. The method is capable to retrieve LST with a precision of ±0.2 °C and LSE with a precision better than ±0.005 for the SEVIRI atmospheric window channels (Masiello et al., 2013). The time dimension Kalman filter approach, after being validated over a variety of surface conditions, is now being considered to become operational within EUMETSAT SEVIRI full-disk level 2 products service (Serio et al., 2014).

Fig. 4 contains the pre-launch spectral response of SEVIRI. Cloud masking was performed by applying an improved version of the SEVIRI operational cloud mask, which considers an additional cloud test that exploits the expected time continuity in the clear sky of SEVIRI radiance at 12 μm. Accordingly, only clear sky conditions were analyzed.

The average LSE for each pixel over time, in each channel during June and July 2013, was calculated. In addition, a subset of 24 pixels over the research area, 12 on each side of the border, was selected for further analysis (Fig. 5). These pixels were selected through the use of high resolution imagery to make sure that they only contained dunes and that no settlements or agricultural activities were present within their boundaries. Therefore, the pixels represented relatively homogenous regions, and the only cover types were bare sands, biocrusts, and very sparse vegetation (pixels containing ephemeral channels, rock outcrops, and playas were also excluded from the analysis). The footprint of each pixel in this area was about 18 km^2.

The cloud masking resulted in gaps within the time series. A total of nine days, for which data were available from most pixels on both sides

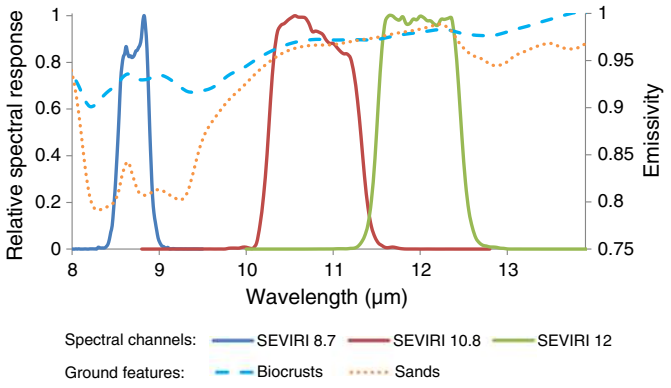

Fig. 4. Pre-launch relative spectral response of the SEVIRI channels imposed over typical spectral emissivity signatures of biocrusts and bare sands that were measured in the field.

of the border at most times, were selected and analyzed (Fig. 3). When less than half of the pixels in each group contained data at a given time, this point in time was excluded from the dataset, resulting in some data gaps in the selected days. This precaution ensured that the final dataset analyzed was reliable. The daily ranges of LST and LSE were computed for each of the selected pixels on the selected days. T-tests for paired samples were conducted to determine whether the daily ranges of LST and LSE in Sinai and the Negev were significantly different.

2.5. Dewpoint computation

In the summer, no precipitation or fog usually occur in the study area. Hence, changes in the soil water content can only be the result of water vapor adsorption or dew formation in combination with evaporation (Agam and Berliner, 2006). In order to assess whether dew could form on the surface, the dew point temperature (T_d) in the study area was calculated by (Lawrence, 2005):

$$T_d = \frac{B_1\left[\ln\left(\frac{e_a}{e_s}\right) + \frac{A_1 T_a}{B_1 + T_a}\right]}{A_1 - \ln\left(\frac{e_a}{e_s}\right) - \frac{A_1 T_a}{B_1 + T_a}} \quad (1)$$

where e_a and e_s are the actual water vapor pressure and the saturated water vapor pressure in the air (mb), respectively, T_a is the air temperature (°C), and $A_1 = 17.625$ and $B_1 = 243.04$ °C were evaluated by Alduchov and Eskridge (1996).

For dew to form, the surface temperature needs to be equal to or lower than the dew point temperature. Subsequently, T_d was compared to the LST in the selected pixels, to determine whether dew formation occurred.

3. Results

Representative spectral signatures of sands and biocrusts measured in the field are presented in Fig. 4. The average June–July LSE values in the SEVIRI 10.8 and 12 μm channels did not show any informative spatial patterns. This was expected since the emissivity values of biocrusts and sands in these channels are similar. However, the 8.7 μm channel exhibited a clear delineation of the dune field boundary and of the political border between Egypt and Israel (Fig. 6). This was due to the distinct quartz doublet absorption feature around 8.25–9.25 μm, which was attenuated by the biocrust cover, and was nearly absent in rock outcrops, soils, and vegetation around the dune field (Rozenstein and Karnieli, 2015). Fig. 7 displays the diurnal dynamics of LST and LSE on June 1, 2013, as an example of the variations on a typical summer day. The LSE behavior in all channels had a v-notch shape, with a minimum corresponding to the LST peak. The variation range in the 8.7 μm channel was one order of magnitude larger than those in the 10.8 and 12 μm channels. The same observation held true for all nine analyzed days. This variation was likely caused by changes in the soil water content. The LST in the selected pixels was found to be consistently above the dew point throughout the research period. Therefore, it was inferred that the dominant mechanism responsible for the diurnal soil moisture dynamics, and thus the LSE variations, was direct adsorption of atmospheric water vapor, rather than dew formation.

Significant differences were found between Sinai and the Negev in all four variables (LSE in three channels and LST, depicted in Fig. 8). In accordance with previous studies (Qin et al., 2002b, 2005), the LST diurnal variation in the Negev was found to be greater than in Sinai (Fig. 8A). The LSE variation in the 8.7 μm channel was also found to be greater in the Negev than in Sinai (Fig. 8B), indicating larger diurnal variations in soil moisture in biocrusts than in sands. However, in the 10.8 and

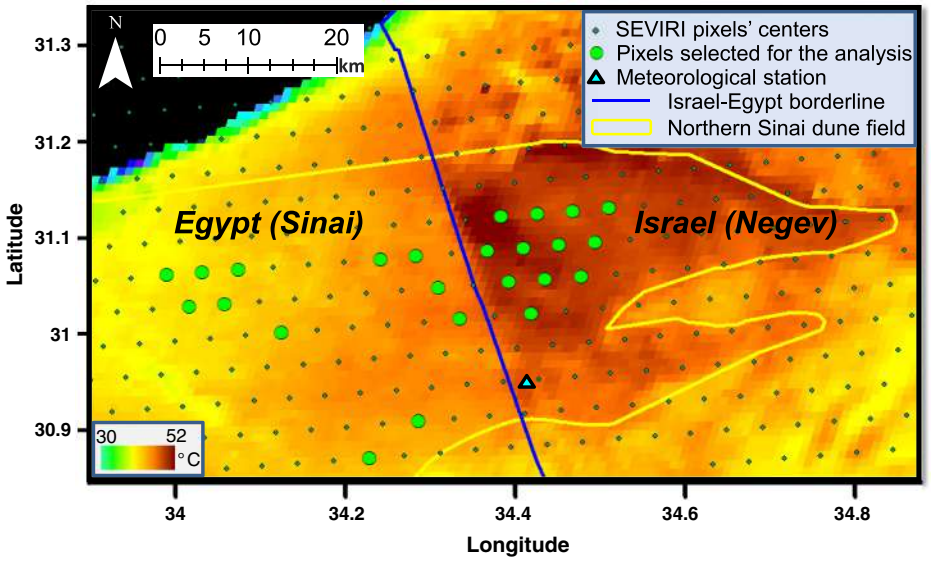

Fig. 5. Terra/MODIS daytime land surface temperature of the research site (MOD11A1) acquired on June 3, 2013. The Israel–Egypt borderline is evident from the sharp temperature contrast between the Negev and Sinai. This contrast is the result of different land-use management: in the Negev, the prohibition of anthropogenic pressures has facilitated biocrust establishment, which has resulted in dune stabilization, while in Sinai, continued grazing and trampling by herds of herbivores have prevented biocrust establishment, maintaining a bare and an active sand dune field.

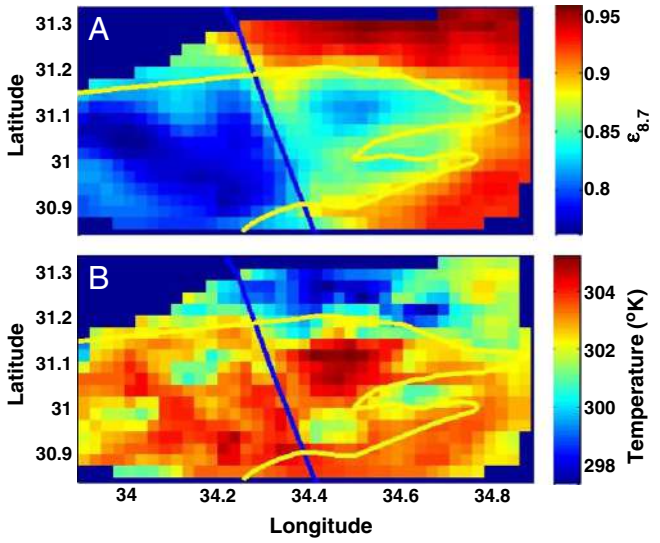

Fig. 6. A) Land surface emissivity in the 8.7 μm SEVIRI channel, and B) land surface temperature, averaged over June–July 2013, over the research area. The Israel–Egypt borderline and the outline of the dune field, which appeared on Figs. 1 and 5 are superimposed on these land surface products. Notice the clear boundary of the dune field in the Negev and the distinct emissivity contrast between dunes in Sinai and the Negev.

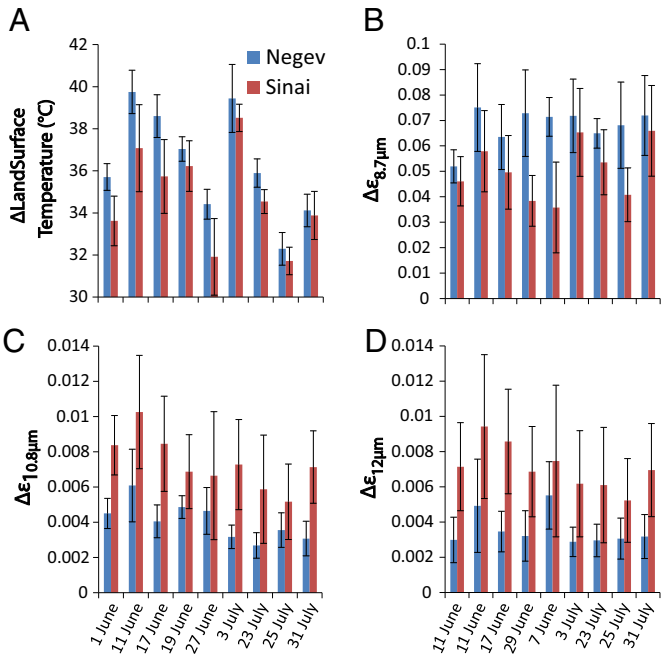

Fig. 8. The daily range of variations in land surface temperature and emissivity for nine selected days. The error bars represent the standard deviation. T-tests for paired samples were conducted, and highly significant differences between the Negev and Sinai were found, with p-value < 0.001 for all four variables.

12 μm channels (Fig. 8C and D) this pattern is reversed: the daily variation range was larger in Sinai than in the Negev. These LSE variations in the 10.8 and 12 μm channels are within 0.001, which is one order of magnitude less than those at 8.7 μm. Since the LSE of sands and biocrusts at 10.8 and 12 μm are high relative to the LSE at 8.7 μm, they are less prone to variations due to changes in soil moisture content. At large viewing angles, the emissivity of water may be lower (Sobrino and Cuenca, 1999), resulting in lower LSE fluctuations when moisture is adsorbed or evaporated from the soil. Since the SEVIRI observations of the research area are made at an angle of about 53°–54°, and since at this large viewing angle the surface could show non-Lambertian effects (García-Santos et al., 2012), the difference in LSE variation between the two sides of the border could be, in part, attributed to the combination of these two effects and the anisotropy of optical and structural properties of the surface.

4. Discussion

Similar to previous studies conducted over the Sahara Desert (Li et al., 2012; Masiello et al., 2013, 2014), the SEVIRI data analysis over the Sinai–Negev area confirmed that there are daily variations in LSE. Additionally, this study was able to demonstrate for the first time that there are differences in the daily LSE variations between sand dunes fixed by biocrusts and bare sands. These differences in daily LSE variations are likely attributed to differences in the daily soil moisture variations, which are created by the larger adsorption of atmospheric water vapor by biocrusts than by bare sands. Although the adsorption of atmospheric water vapor by the soil surface changes the soil moisture by very

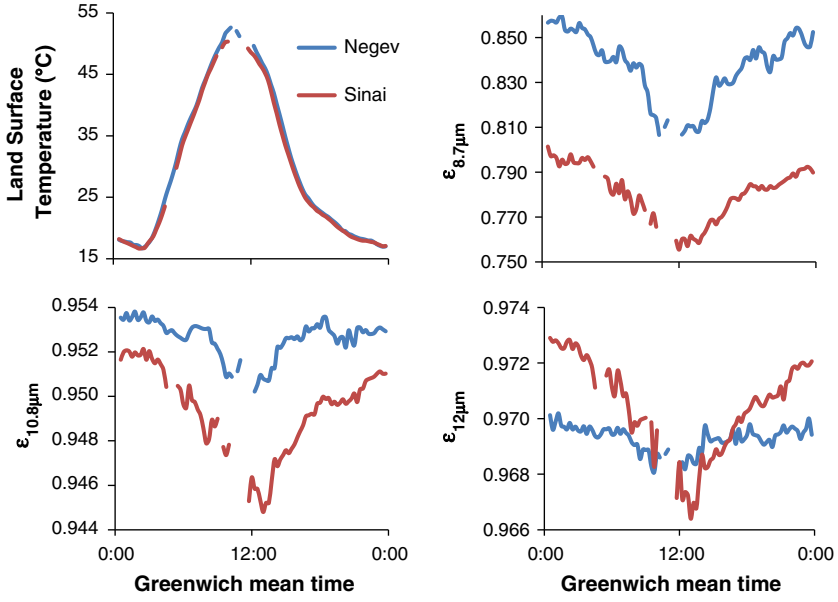

Fig. 7. The diurnal dynamics of temperature and emissivity on June 1, 2013. Gaps in the graph are the result of missing data due to clouds. Notice that the variation range in the 8.7 μm channel was one order of magnitude larger than those in the 10.8 and 12 μm channels.

small amounts, this process has a wide spatial expression and is detectable by satellite remote sensing.

This discovery may have consequences for model estimates of LST and ground fluxes, as previously demonstrated by Agam et al. (2004). Not accounting for the soil moisture effect on LSE may introduce bias into LST estimations. For instance, split window algorithms that use LSE estimates do not account for diurnal emissivity variations or for differences in the diurnal variation between similar land-cover types (Jiang and Li, 2008; Rozenstein et al., 2014a; Wan and Dozier, 1996). It is common for LSE estimations to be derived from remote sensing images acquired during the daytime. Furthermore, LSE is often obtained from a land-cover classification based on reflective bands, in which the emissivity values for each class are assumed (Snyder et al., 1998). This type of approach is exercised for the Moderate Resolution Imaging Spectroradiometer (MODIS) LST and LSE products (*e.g.* MOD11). The MODIS LSE estimates are often inaccurate for arid and semiarid areas (Göttsche and Hulley, 2012; Hulley and Hook, 2009), which could be partly attributed to the day–night variations in soil moisture. Furthermore, land-cover classification, based on emissivity estimates, might not be sensitive to subtle differences, such as bare *vs.* biocrusted dunes, and thus not take into account the difference in soil moisture dynamics between these two land-cover types. Estimating the magnitude of potential errors in various LST and flux models is outside the scope of the current investigation.

While the difference in diurnal topsoil LSE dynamics between sands and biocrusts was demonstrated for the Sinai–Negev area, these findings could be applicable for many other deserts where sands are covered, to some extent, by biocrusts and coupled with a source of atmospheric moisture. In such environments, it can be expected that similar differences in the dynamics of soil moisture and, consequently, of LSE will be found between sands stabilized by biocrusts and bare sands. Therefore, these findings may be relevant for all of the fringe areas around the Sahara Desert, the Arabian Peninsula, the west coast of southern Africa, the Central Asian ergs, and sandy areas in Australia, Brazil, and North America. The next phase in studying this phenomenon should include calibrating the spaceborne observations of diurnal LSE variations against simultaneous ground measurements of the topsoil moisture dynamics. This should be performed in a site-specific manner, since both the sand and biocrust compositions differ from place to place, and thus, the spectral LSE is expected to be different. Additional variability within each pixel must also be accounted for, since additional spectrally flat components, such as vegetation, as well as variations in sand particle size, organic matter content, and mineralogy (*e.g.*, clays, magnetite, and hematite) may influence the pixels' LSE (Hulley et al., 2010; Salisbury and D'Aria, 1992) and, subsequently, affect the LSE's diurnal dynamics. Another way forward is to apply physically-based algorithms to retrieve LST and LSE simultaneously from LWIR sensors (*e.g.* Gillespie et al., 1998), which will dynamically take into account any soil moisture changes in LSE. This has been applied to MODIS starting with Collection 6 data through the new MOD21 product (Hulley et al., 2014).

5. Conclusions

LSE dynamics were determined from geostationary orbit by SEVIRI over a coastal desert, where diurnal variations in the soil moisture, due to the adsorption of water vapor from the sea breeze and its consequent evaporation, were reported. These dynamics differed across the two dune environments where contrasting land-use practices resulted in bare sands in one region and dunes fixed by biocrusts in the other. The surface area of biocrusts, containing larger clay content, is greater than that of bare sands. Therefore, biocrusts adsorb more water vapor than do sands. Consequently, the SEVIRI LSEs showed larger diurnal variations in the 8.7 μm channel for the dunes fixed by biocrusts than in the active dunes. These differences in diurnal LSE variation should be accounted for in geophysical models that rely on LSE input. Since biocrusts cover vast desert regions worldwide, LSE variations potentially have a considerable effect on model predictions from the local to the global scale.

Acknowledgments

The project was funded by the Israeli Ministry of Science and Technology. Offer Rozenstein was supported by the Pratt Foundation. We thank Prof. Yosef Ashkenazy of the Blaustein Institutes for Desert Research, Ben-Gurion University of the Negev, for sharing data from the meteorological station at the Nizzana research site.

References

Agam N, Berliner PR. Diurnal water content changes in the bare soil of a coastal desert. J Hydrometeorol 2004;5:922–33.
Agam N, Berliner PR. Dew formation and water vapor adsorption in semi-arid environments — a review. J Arid Environ 2006;65:572–90.
Agam N, Berliner PR, Zangvil A, Ben-Dor E. Soil water evaporation during the dry season in an arid zone. J Geophys Res 2004;109:D16103.
Alduchov OA, Eskridge RE. Improved magnus form approximation of saturation vapor pressure. J Appl Meteorol 1996;35:601–9.
Becker F, Li ZL. Temperature-independent spectral indexes in thermal infrared bands. Remote Sens Environ 1990;32:17–33.
Belnap J. Microphytic crust: 'topsoil' of the desert. Permac Drylands J 1990;10:4. [5, 14].
Belnap J. The potential roles of biological soil crusts in dryland hydrologic cycles. Hydrol Process 2006;20:3159–78.
Belnap J, Lange OL. Biological soil crusts: structure, function, and management, 150; 2001. p. 503.
Clerbaux C, Hadji-Lazaro J, Turquety S, Megie G, Coheur PF. Trace gas measurements from infrared satellite for chemistry and climate applications. Atmos Chem Phys 2003;3:1495–508.
Danin A, Ganor E. Trapping of airborne dust by mosses in the Negev Desert, Israel. Earth Surf Process Landf 1991;16:153–62.
Felde V, Peth S, Uteau-Puschmann D, Drahorad S, Felix-Henningsen P. Soil microstructure as an under-explored feature of biological soil crust hydrological properties: case study from the NW Negev Desert. Biodivers Conserv 2014;23:1687–708.
French AN, Schmugge TJ, Ritchie JC, Hsu A, Jacob F, Ogawa K. Detecting land cover change at the Jornada Experimental Range, New Mexico with ASTER emissivities. Remote Sens Environ 2008;112:1730–48.
García-Santos V, Valor E, Caselles V, Ángeles Burgos M, Coll C. On the angular variation of thermal infrared emissivity of inorganic soils. J Geophys Res Atmos 2012;117:D19116.
Gillespie A, Rokugawa S, Matsunaga T, Cothern JS, Hook S, Kahle AB. A temperature and emissivity separation algorithm for Advanced Spaceborne Thermal Emission and Reflection Radiometer (ASTER) images. IEEE Trans Geosci Remote Sens 1998;36:1113–26.
Göttsche F, Hulley GC. Validation of six satellite-retrieved land surface emissivity products over two land cover types in a hyper-arid region. Remote Sens Environ 2012;124:149–58.
Hulley GC, Hook SJ. Intercomparison of versions 4, 4.1 and 5 of the MODIS Land Surface Temperature and Emissivity products and validation with laboratory measurements of sand samples from the Namib Desert, Namibia. Remote Sens Environ 2009;113:1313–8.
Hulley GC, Hook SJ, Baldridge AM. Investigating the effects of soil moisture on thermal infrared land surface temperature and emissivity using satellite retrievals and laboratory measurements. Remote Sens Environ 2010;114:1480–93.
Hulley G, Veraverbeke S, Hook S. Thermal-based techniques for land cover change detection using a new dynamic MODIS multispectral emissivity product (MOD21). Remote Sens Environ 2014;140:755–65.
Immerzeel WW, Droogers P. Calibration of a distributed hydrological model based on satellite evapotranspiration. J Hydrol 2008;349:411–24.
Jiang G, Li Z. Split-window algorithm for land surface temperature estimation from MSG1-SEVIRI data. Int J Remote Sens 2008;29:6067–74.
Karnieli A, Dall'Olmo G. Remote-sensing monitoring of desertification, phenology, and droughts. Manag Environ Qual Int J 2003;14:22–38.
Karnieli A, Tsoar H. Satellite spectral reflectance of biogenic crust developed on desert dune sand along the Israel–Egypt border. Int J Remote Sens 1995;16:369–74.
Karnieli A, Shachak M, Tsoar H, Zaady E, Kaufman Y, Danin A, et al. The effect of microphytes on the spectral reflectance of vegetation in semiarid regions. Remote Sens Environ 1996;57:88–96.
Kuske CR, Yeager CM, Johnson S, Ticknor LO, Belnap J. Response and resilience of soil biocrust bacterial communities to chronic physical disturbance in arid shrublands. ISME J 2012;6:886–97.
Lawrence MG. The relationship between relative humidity and the dewpoint temperature in moist air: a simple conversion and applications. Bull Am Meteorol Soc 2005;86:225–33.
Li J, Zhang P, Schmit TJ, Schmetz J, Menzel WP. Quantitative monitoring of a Saharan dust event with SEVIRI on Meteosat-8. Int J Remote Sens 2007;28:2181–6.
Li Z, Li J, Li Y, Zhang Y, Schmit TJ, Zhou L, et al. Determining diurnal variations of land surface emissivity from geostationary satellites. J Geophys Res 2012;117:D23302.
Li Z, Wu H, Wang N, Qiu S, Sobrino JA, Wan Z, et al. Land surface emissivity retrieval from satellite data. Int J Remote Sens 2013a;34:3084–127.

Li Z, Tang B, Wu H, Ren H, Yan G, Wan Z, et al. Satellite-derived land surface temperature: current status and perspectives. Remote Sens Environ 2013b;131:14–37.
Liu L, Li S, Duan Z, Wang T, Zhang Z, Li X. Effects of microbiotic crusts on dew deposition in the restored vegetation area at Shapotou, Northwest China. J Hydrol 2006;328:331–7.
Masiello G, Serio C. Simultaneous physical retrieval of surface emissivity spectrum and atmospheric parameters from infrared atmospheric sounder interferometer spectral radiances. Appl Opt 2013;52:2428–46.
Masiello G, Serio C, De Feis I, Amoroso M, Venafra S, Trigo IF, et al. Kalman filter physical retrieval of surface emissivity and temperature from geostationary infrared radiances. Atmos Meas Tech 2013;6:3613–34.
Masiello G, Serio C, Venafra S, DeFeis I, Borbas EE. Diurnal variation in Sahara desert sand emissivity during the dry season from IASI observations. J Geophys Res 2014;119:1626–38.
Mira M, Valor E, Boluda R, Caselles V, Coll C. Influence of soil water content on the thermal infrared emissivity of bare soils: implication for land surface temperature determination. J Geophys Res 2007;112:F04003.
Mira M, Valor E, Caselles V, Rubio E, Coll C, Galve JM, et al. Soil moisture effect on thermal infrared (8–13-μm) emissivity. IEEE Trans Geosci Remote Sens 2010;48:2251–60.
Ogawa K, Schmugge T, Rokugawa S. Estimating broadband emissivity of arid regions and its seasonal variations using thermal infrared remote sensing. IEEE Trans Geosci Remote Sens 2008;46:334–43.
Pan Y, Wang X, Zhang Y. Dew formation characteristics in a revegetation-stabilized desert ecosystem in Shapotou area, Northern China. J Hydrol 2010;387:265–72.
Philip J, De Vries D. Moisture movement in porous materials under temperature gradients. Trans Am Geophys Union 1957;38:222–32.
Puckrin E, Moreau L, Bourque H, Ouellet R, Prel F, Roy C, et al. A broadband field portable reflectometer to characterize soils and chemical samples. SPIE Defense, Security, and Sensing; 2013. p. 870917. [870917-11].
Qin Z, Berliner P, Karnieli A. Micrometeorological modeling to understand the thermal anomaly in the sand dunes across the Israel–Egypt border. J Arid Environ 2002a;51:281–318.
Qin Z, Karnieli A, Berliner P. Remote sensing analysis of the land surface temperature anomaly in the sand-dune region across the Israel–Egypt border. Int J Remote Sens 2002b;23:3991–4018.
Qin Z, Berliner P, Karnieli A. Ground temperature measurement and emissivity determination to understand the thermal anomaly and its significance on the development of an arid environmental ecosystem in the sand dunes across the Israel–Egypt border. J Arid Environ 2005;60:27–52.
Ram A, Aaron Y. Negative and positive effects of topsoil biological crusts on water availability along a rainfall gradient in a sandy arid area. Catena 2007;70:437–42.
Rao B, Liu Y, Wang W, Hu C, Dunhai L, Lan S. Influence of dew on biomass and photosystem II activity of cyanobacterial crusts in the Hopq Desert, Northwest China. Soil Biol Biochem 2009;41:2387–93.
Roskin J, Blumberg DG, Porat N, Tsoar H, Rozenstein O. Do dune sands redden with age? The case of the northwestern Negev dunefield, Israel. Aeolian Res 2012;5:63–75.
Rozenstein O, Karnieli A. Identification and characterization of biological soil crusts in a sand dune desert environment across Israel–Egypt border using LWIR emittance spectroscopy. J Arid Environ 2015;112, Part A:75–86.
Rozenstein O, Qin Z, Derimian Y, Karnieli A. Derivation of land surface temperature for Landsat-8 TIRS Using a split window algorithm. Sensors 2014a;14:5768–80.
Rozenstein O, Zaady E, Katra I, Karnieli A, Adamowski J, Yizhaq H. The effect of sand grain size on the development of cyanobacterial biocrusts. Aeolian Res 2014b;15:217–26.
Salisbury JW, D'Aria DM. Infrared (8–14 μm) remote sensing of soil particle size. Remote Sens Environ 1992;42:157–65.
Sanchez JM, French AN, Mira M, Hunsaker DJ, Thorp KR, Valor E, et al. Thermal infrared emissivity dependence on soil moisture in field conditions. IEEE Trans Geosci Remote Sens 2011;49:4652–9.
Seemann SW, Borbas EE, Knuteson RO, Stephenson GR, Huang Hung-Lung. Development of a global infrared land surface emissivity database for application to clear sky sounding retrievals from multispectral satellite radiance measurements. J Appl Meteorol Climatol 2008;47:108–23.
Serio C, Liuzzi G, Masiello G, Venafra S, De Feis I. Kalman filter estimation of surface temperature and emissivity from SEVIRI: final report. Technical memorandumEUMETSAT project EUM/CO/14/4600001329/PDW; 2014. p. 1–65.
Siegal Z, Tsoar H, Karnieli A. Effects of prolonged drought on the vegetation cover of sand dunes in the NW Negev Desert: field survey, remote sensing and conceptual modeling. Aeolian Res 2013;9:161–73.
Snyder WC, Wan Z, Zhang Y, Feng Y-. Classification-based emissivity for land surface temperature measurement from space. Int J Remote Sens 1998;19:2753–74.
Sobrino JA, Cuenca J. Angular variation of thermal infrared emissivity for some natural surfaces from experimental measurements. Appl Opt 1999;38:3931–6.
Tsoar H, Karnieli A. What determines the spectral reflectance of the Negev–Sinai sand dunes. Int J Remote Sens 1996;17:513–25.
Tsoar H, Blumberg DG, Wenkart R. Formation and geomorphology of the north-western Negev sand dunes. In: Breckle S, Yair A, Veste M, editors. Arid dune ecosystems: the Nizzana Sands in the Negev Desert. Springer Berlin Heidelberg; 2008. p. 25–48.
Veste M, Littmann T, Breckle S-, Yair A. The role of biological soil crusts on desert sand dunes in the northwestern Negev, Israel. In: Breckle S-, Veste M, Wucherer W, editors. Sustainable land use in deserts. Berlin: Springer; 2001. p. 357–67.
Wan Zhengming, Dozier J. A generalized split-window algorithm for retrieving land-surface temperature from space. IEEE Trans Geosci Remote Sens 1996;34:892–905.
Zaady E, Offer ZY. Biogenic soil crusts and soil depth: a long-term case study from the central Negev desert highland. Sedimentology 2010;57:351–8.
Zhang P, Lu N, Hu X, Dong C. Identification and physical retrieval of dust storm using three MODIS thermal IR channels. Global Planet Chang 2006;52:197–206.
Zhang J, Zhang Y, Downing A, Cheng J, Zhou X, Zhang B. The influence of biological soil crusts on dew deposition in Gurbantunggut Desert, Northwestern China. J Hydrol 2009;379:220–8.
Zhou L, Dickinson R, Tian Y, Jin M, Ogawa K, Yu H, et al. A sensitivity study of climate and energy balance simulations with use of satellite-derived emissivity data over Northern Africa and the Arabian Peninsula. J Geophys Res 2003;108:4795.